

Nuclear-magnetic-resonance study of the magnetically ordered manganite

$\text{La}_{1-x}\text{Pb}_x\text{Mn}_{1-y}\text{Fe}_y\text{O}_3$

L. K. Leung* and A. H. Morrish

Department of Physics, University of Manitoba, Winnipeg, Canada R3T 2N2

(Received 16 August 1976)

A study of the manganite, $\text{La}_{1-x}\text{Pb}_x\text{Mn}_{1-y}\text{Fe}_y\text{O}_3$, where $0.25 < x < 0.45$ and $0.0 \leq y \leq 0.17$, has been made using the pulsed nuclear-magnetic-resonance technique over the temperature range from 1.6 to 77 K. Multiple spin echoes have been observed for ^{55}Mn nuclei in the ferromagnet $\text{La}_{1-x}\text{Pb}_x\text{MnO}_3$; their number is consistent with refocusing by the quadrupole interaction. The NMR spectra have broad linewidths; experiments with a magnetic field applied indicate that nuclei both within domain walls, and within the domain bulk, contribute significantly to the absorption. The resonance frequency, defined by the signal maximum, is proportional to the average spin $\langle S \rangle$, which in turn is a function of composition, as well as temperature. The spin-spin relaxation time T_2 is a minimum at the resonance frequency when $T = 4.2$ K; the Suhl-Nakamura interaction is suggested to be the predominant mechanism acting. The spin-echo amplitude is an oscillatory function of the time between the two exciting pulses; from these data the quadrupole splitting (e^2qQ/h) is deduced to be about 0.17 MHz. When some of the manganese is replaced by iron, two additional peaks, one on the low- and the other on the high-frequency side, appear in the NMR spectra, and are attributed to localized Mn^{4+} and Mn^{3+} ions, respectively. The implications of increased electron localization at the manganese ions for the magnetization of $\text{La}_{1-x}\text{Pb}_x\text{Mn}_{1-y}\text{Fe}_y\text{O}_3$ are discussed.

I. INTRODUCTION

A series of experiments at the University of Manitoba has established that the manganites $\text{La}_{1-x}\text{Pb}_x\text{MnO}_3$, with $0.25 < x < 0.45$, are ferromagnets.¹⁻³ Also, the change in the magnetic structure when some manganese is replaced by iron has been the subject of a recent report.⁴ These investigations have now been extended to a study of nuclear magnetic resonance of the isotope ^{55}Mn in these compounds.

The ferromagnetism of $(\text{LaPb})\text{MnO}_3$ has its origin in the coupling between the manganese ions produced by a narrow double-exchange band occupied by $1-x$ electrons per formula unit.⁵ This interaction is comparatively large, and leads to Curie temperatures T_f , between 320 and 350 K. Although the theory of the double-exchange interaction dates back to the early 1950's, the literature on this subject is not extensive.⁶

The iron-doped compounds $\text{La}_{1-x}\text{Pb}_x\text{Mn}_{1-y}\text{Fe}_y\text{O}_3$, with $0.03 \leq y \leq 0.17$, have lower magnetizations and Curie temperatures. Mössbauer spectra establish that the iron ions are in the high-spin Fe^{3+} state, and couple antiferromagnetically to the manganese ions. Both the Fe-O-Mn and Fe-O-Fe superexchange interactions play a role in determining the magnetic structure.⁴

Measurements had been made earlier of the static magnetization,^{2,4} ferromagnetic resonance absorption,³ electrical resistivity including magnetoresistance,⁵ lattice parameters,^{1,4} and, for the samples doped with ^{57}Fe , Mössbauer spectra.⁴

More recently, data have been obtained on x-ray and uv photoemission.⁷ This is the first report on the nuclear magnetic resonance of the $\text{La}_{1-x}\text{Pb}_x\text{Mn}_{1-y}\text{Fe}_y\text{O}_3$ family; however, there have been papers on NMR absorption in two related compounds. NMR signals were observed by the spin-echo technique from the perovskite ferromagnet $\text{La}_{0.70}\text{Sr}_{0.30}\text{MnO}_3$. There were maxima at about 374 and 382 MHz, and, although the authors were somewhat uncertain as to their origin, at least one absorption was ascribed to the nucleus ^{55}Mn .⁸ With the same technique, Matsumoto⁹ observed ^{55}Mn NMR spectra for $\text{La}_{1-x}\text{Ca}_x\text{MnO}_3$ with $0.125 \leq x \leq 0.3$ down to temperatures as low as 1.4 K. For $x \leq 0.175$, a peak at 323 MHz is ascribed to Mn^{4+} ions, and a broad absorption, ranging from 350 to 435 MHz, to Mn^{3+} ions, with motional narrowing, by the double-exchange electrons. Actually, for $x = 0.15$ at $T = 4.2$ K, there is a maximum at 411 MHz, which may be the resonance of Mn^{3+} ions, and a subsidiary peak at about 380 MHz, which may be related to $\text{Mn}^{3.15+}$ ions. The spin-echo decay time T_2^* was found to be 10 μsec for the Mn^{4+} absorption and 4 μsec for the absorption at 378 MHz, both for $x = 0.15$ at $T = 4.2$ K. For $x = 0.2$ and 0.3, only one motionally narrowed absorption was observed, with a maximum at 378 MHz at $T = 4.2$ K, and presumably corresponds to $\text{Mn}^{(3+x)+}$ ions. The hyperfine constant A was determined to be $|A| = 72 \times 10^{-4} \text{ cm}^{-1}$ for the Mn^{4+} ions. No multiple echoes were observed at $T = 77$ K, and if they were observed at lower temperatures, they were not reported.

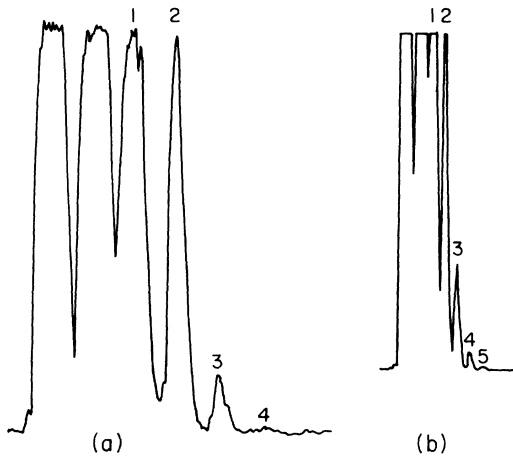


FIG. 1. Pen recorder traces of multiple spin-echo NMR signals for $\text{La}_{1-x}\text{Pb}_x\text{MnO}_3$ at $T=1.6$ K (a) for $x=0.31$ with $\tau=2$ μsec and (b) for $x=0.26$ with $\tau=1$ μsec .

II. NMR SPIN-ECHO EXPERIMENTS ON $(\text{LaPb})\text{MnO}_3$

A variable-frequency incoherent-pulse spectrometer was used in the experiments.¹⁰ The tail of a glass Dewar containing the sample was inserted through an aperture into the cavity. By pumping on the liquid helium, temperatures down to 1.6 K were achieved.¹¹

Usually the $(\text{La}_{1-x}\text{Pb}_x)\text{MnO}_3$ samples were powders obtained by crushing single crystals. These powders were introduced into a quartz tube to form a cylindrically shaped sample. A few spherical-shaped single crystals were investigated. However, the skin depth $\delta_0(=2\epsilon_0 c^2/\sigma\omega)^{1/2}$ when $\omega \approx 2\pi \times 400$ MHz and $\sigma \approx 10^2(\Omega \text{ cm})^{-1}$ is about 0.26 mm. Since the diameter of the single crystals, about 1 mm, was larger than δ , the amplitude of the signal was then reduced.

Most of the measurements were made on samples with $x=0.26$, 0.31, and 0.40 at temperatures of 77, 4.2, and 1.6 K. A single echo, similar to that reported by Matsumoto⁹ for $(\text{LaCa})\text{MnO}_3$, was observed at $T=77$ K. However, at $T=4.2$ K, multiple echoes were observed, for example four for $x=0.26$. The maximum number of echoes was detected at 1.6 K, five for $x=0.26$ and four for $x=0.31$, as illustrated in Fig. 1.

The phenomenon of multiple-spin echoes that occur at 2τ , 3τ , ..., where τ is the time interval between the two exciting pulses, has been observed earlier in many magnetic materials.^{3,12,13} When the refocusing mechanism for the second and any subsequent echoes is the quadrupole interaction, a maximum of $2I$ echoes is predicted by theory.¹³ Since $I=\frac{5}{2}$ for ^{55}Mn , the present observations seem to imply that the quadrupole in-

teraction is the source of the multiple echoes in $(\text{LaPb})\text{MnO}_3$. However, it is possible that observations at even lower temperatures, or with increased amplifier gain, might reveal more than five echoes. If the number of echoes exceeds $2I$, a coupling between the nuclear spins via emission and absorption of virtual spin waves, the Suhl-Nakamura interaction, is probably the source of the refocusing.¹⁰ Therefore, although it is concluded that the quadrupole interaction is the origin of the multiple echoes, it cannot be ruled out that the Suhl-Nakamura interaction is partially, or even entirely, the mechanism operating.

The amplitude of an echo is expected to be proportional to $e^{-2\tau/T_2}$, where T_2 is the transverse or spin-spin relaxation time. However, T_2 is itself a function of frequency. The data had therefore to be taken by varying τ in such a way that τ/T_2 was kept constant. Since the power output of the oscillator and the receiver gain were not constant as the frequency was changed, the collection of accurate data was not easy. The NMR spectra at $T=4.2$ K are illustrated for three values of x in Fig. 2; in addition one spectrum for $T=77$ K is shown. The spectra are broad, with an average halfwidth (width at half-maximum) of about 34 MHz, and essentially independent of temperature. Thus, the line must be inhomogeneous.

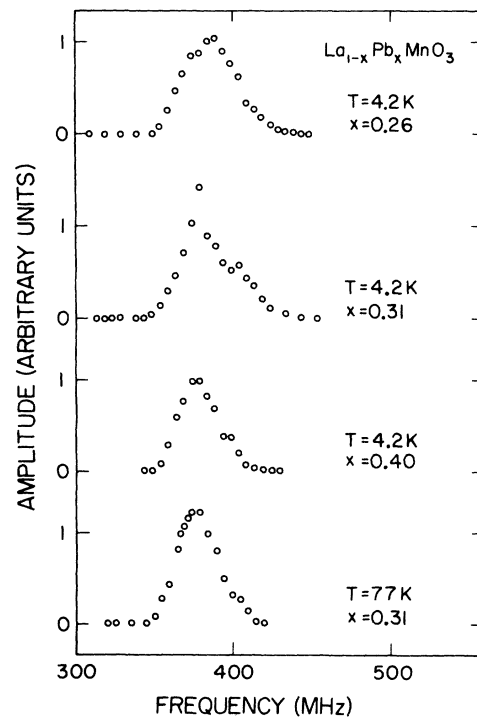


FIG. 2. NMR spectra of $\text{La}_{1-x}\text{Pb}_x\text{MnO}_3$ for $x=0.26$, 0.31, and 0.40 at $T=4.2$ K and for $x=0.31$ at $T=77$ K.

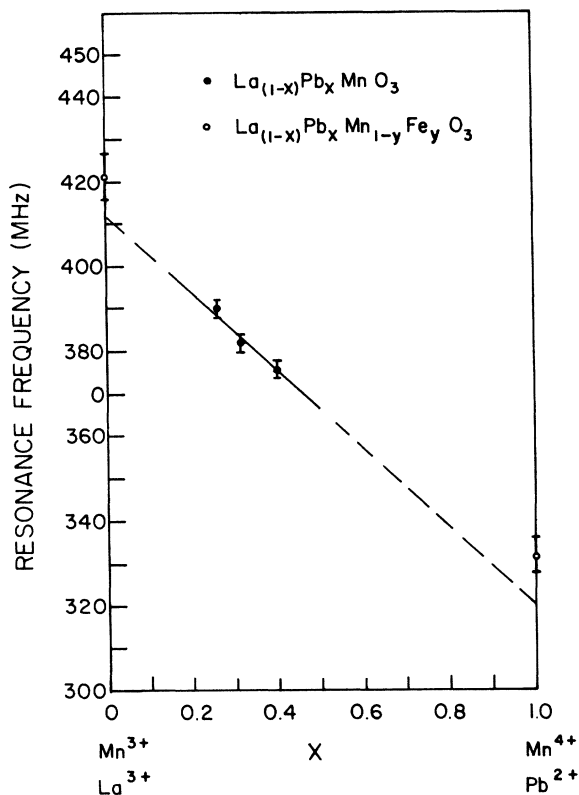


FIG. 3. Resonance frequency of $\text{La}_{1-x}\text{Pb}_x\text{MnO}_3$ as a function of composition at $T = 4.2$ K. The frequency of the peaks associated with Mn^{3+} and Mn^{4+} ions in $\text{La}_{1-x}\text{Pb}_x\text{Mn}_{1-y}\text{Fe}_y\text{O}_3$ at $T = 1.6$ K are also plotted.

generously broadened. The maximum amplitude will be used to define the resonance frequency ν_0 . The values of ν_0 obtained from the data of Fig. 2 are plotted as a function of x in Fig. 3 for $T = 4.2$ K; within the experimental errors ν_0 is a linear function of the degree of ionization of the manganese.

Resonance frequencies are also listed in Table I. It should be recalled that Matsumoto found $\nu_0 \approx 380$ MHz for $\text{La}_{1-x}\text{Ca}_x\text{MnO}_3$ with $x = 0.2$ and 0.3 at $T = 4.2$ K;⁹ the resonance frequencies for the calcium and lead manganites are thus remarkably similar. In addition, the average spin per formula unit, $\langle S \rangle$, are given. For $T = 4.2$ K, $\langle S \rangle$ is the mean value deduced from (a) the chemical formula, (b) the magnetization, and (c) the Curie constant. As reported in an earlier publication,² the largest difference between any two values of $\langle S \rangle$ of a given composition is 3%; most values agree to within 1%. Therefore, provided the magnetic structure is collinear, it follows from these data that there is no appreciable orbital contribution to the magnetic moment. For $T = 77$ K,

$\langle S \rangle$ is deduced from the magnetization measured at this temperature.² The hyperfine coupling may be expressed by $A \vec{I} \cdot \vec{S}$, where A , the hyperfine constant, is related to the resonance frequency by the equation $A = h\nu_0 / \langle S \rangle$. Values of $|A|$, in units of cm^{-1} , are listed in Table I for the samples (to obtain A in energy units, multiply by $1/hc$). These values agree internally to better than 1%. The variation of ν_0 observed therefore merely reflects the different magnetization, or $\langle S \rangle$, of the samples. The ^{55}Mn hyperfine coupling constants found for other materials were 7.2×10^{-3} for $(\text{La}_{1-x}\text{Ca}_x)\text{MnO}_3$,⁹ 7.0×10^{-3} for $\text{LiMn}_{1.5}\text{Fe}_{3.5}\text{O}_8$,¹⁴ 7.0×10^{-3} for $\text{Al}_2\text{O}_3:\text{Mn}^{4+}$,¹⁵ and 7.2×10^{-3} for $\text{MgO}:\text{Mn}^{4+}$.¹⁶ The first two values were determined by NMR, and the latter two by ESR; all are in respectable agreement with the present results. The hyperfine field at the ^{55}Mn nucleus, H_{hf} , can be found from the relationship $\omega_0 = 2\pi\nu_0 = \gamma_N H_{\text{hf}}$, where γ_N is the gyromagnetic ratio. The hyperfine fields calculated by setting $\gamma_N = 2\pi \times 1055$ (Oe sec^{-1}), the accepted value, are listed in Table I. The ratios $(H_{\text{hf}}/\langle S \rangle)$ lie within 1% of each other, and thus confirm that magnetization differences are the origin of the variation in H_{hf} .

The resonance lines of Fig. 2 are too broad to be used to obtain a measure of the transverse relaxation time T_2 . Instead, pairs of pulses separated by different time intervals τ , were applied repeatedly keeping the rf constant. The logarithm of the amplitude of the first echo plotted as a function of τ is a straight line; the slope then yields a value for T_2 at one frequency. This procedure corresponds to method A discussed by Carr and Purcell.¹⁷ The variation of T_2 with frequency across the line profile for one sample at the temperatures 77 and 4.2 K is shown in Fig. 4. A measurement of T_2 near the resonance frequency ν_0 , at $T = 1.7$ K indicates that T_2 changes but little from that at $T = 4.2$ K.

Above liquid-helium temperatures the spin-spin relaxation time is clearly temperature dependent. At 4.2 K, the minimum in T_2 presumably occurs because the majority of the nuclei precess at or near this frequency. It appears, therefore, that the relaxation is occurring, at least at low temperatures, through some nuclear spin-spin

TABLE I. NMR data for $\text{La}_{1-x}\text{Pb}_x\text{MnO}_3$.

| x | T (K) | ν_0 (MHz) | $\langle S \rangle$ | $ A $ (cm^{-1}) | H_{hf} (kOe) |
|------|---------|---------------|---------------------|----------------------------|-----------------------|
| 0.26 | 4.2 | 390 ± 3 | 1.87 | 6.95×10^{-3} | -370 ± 6 |
| 0.31 | 4.2 | 382 ± 3 | 1.85 | 6.88×10^{-3} | -364 ± 6 |
| 0.40 | 4.2 | 376 ± 3 | 1.83 | 6.85×10^{-3} | -357 ± 6 |
| 0.31 | 77 | 376 ± 3 | 1.83 | 6.85×10^{-3} | -357 ± 6 |

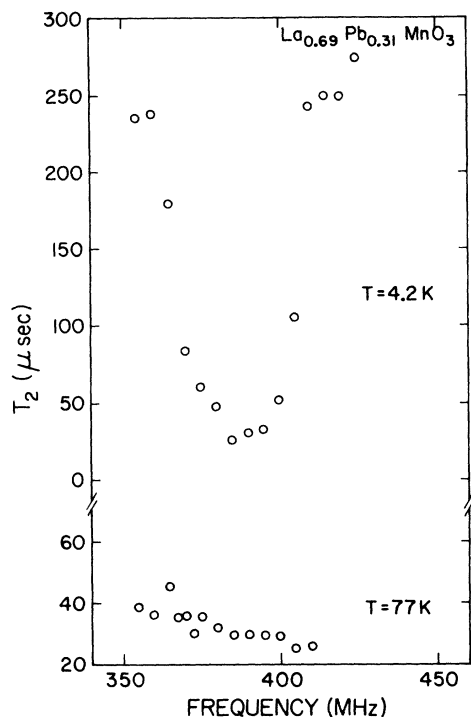


FIG. 4. Spin-spin relaxation time T_2 as a function of frequency for $\text{La}_{0.69}\text{Pb}_{0.31}\text{MnO}_3$ at $T = 4.2$ and 77 K.

interaction. Two possible mechanisms involve spin-waves and wall excitations.¹⁸ Another is the Suhl-Nakamura interaction¹⁹ in which the nuclear spins interact via virtual spin waves in the electronic system. The present observations are qualitatively similar to those found for the ^{55}Mn nuclei of Mn^{2+} ions in manganese ferrite.¹⁰ On the basis of calculations, it was concluded that relaxation in the ferrite was dominated by the Suhl-Nakamura interaction at and below liquid-helium temperatures. Although this interaction was still visible in the form of a shallow minimum at 77 K, it was suggested that the main contribution to T_2 was then a spin-wave scattering process. $(\text{LaPb})\text{MnO}_3$ differs from the ferrite in that the manganese occurs as Mn^{4+} ions together with a narrow double-exchange band. Although it is not clear what complications these factors introduce, the frequency dependence of the spin-spin relaxation time at 4.2 K does suggest that the Suhl-Nakamura interaction plays an important role here too.

III. MAGNETIC FIELD STUDIES

The application of an external magnetic field in spin-echo experiments has the potential to provide additional useful information. For this purpose, a metal Dewar was constructed that could be in-

serted either in an electromagnet (maximum field 18 kOe), or a superconducting solenoid (50 kOe). A cylindrical cavity, sited inside and towards the bottom of the Dewar, had a fixed diameter and a length determined by trial and error. Adjustments were made with a variable capacitor controlled by a long rod protruding through the top of the Dewar.

It seems possible that the large halfwidth of the NMR spectra is at least partially the result of overlapping contributions from nuclei within and outside domain walls. The application of a magnetic field sufficiently large to saturate the sample, that is, remove all the domain walls, should leave only the one contribution, that of nuclei in the bulk material. When fields in the range from 4 to 14 kOe are applied a signal is still observed with a line shape that is more symmetric and a linewidth that is reduced by about half, as illustrated in Fig. 5. We will return to this point when signal amplitudes are discussed at the end of the section.

The resonance frequency is also reduced, as shown in Fig. 6 for $\text{La}_{0.69}\text{Pb}_{0.31}\text{MnO}_3$ at $T = 77$ K. For fields larger than about 10 kOe, the data points lie on a straight line, indicated by the full curve. The slope gives the nuclear gyromagnetic ratio; it is determined to be $\gamma_N \approx 2\pi \times 1000$ $(\text{Oe sec})^{-1}$, which is respectably close to the accepted value of $2\pi \times 1055$ $(\text{Oe sec})^{-1}$. The negative slope indicates that the hyperfine field H_{hf} , is

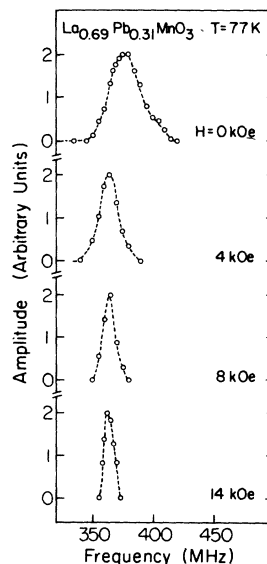


FIG. 5. Resonance spectra of $\text{La}_{0.69}\text{Pb}_{0.31}\text{MnO}_3$ at $T = 77$ K in external magnetic fields. The amplitude of the signal for $H = 14$ kOe is about 3% of that for zero applied field.

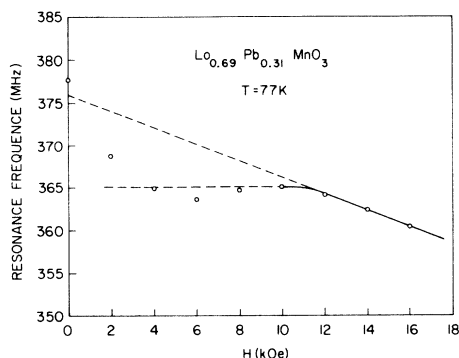


FIG. 6. Resonance frequency ν_0 , as a function of applied external magnetic field for $\text{La}_{0.69}\text{Pb}_{0.31}\text{MnO}_3$ at 77 K. Here ν_0 is defined as corresponding to the maximum amplitude. The full curve fits the data in the region where the sample is magnetically saturated. The upper dashed line is an extrapolation from high fields, and the lower dashed line fits the actual data in the region where domain walls exist.

negative, that is, lies in the direction opposite to that of the electronic magnetization. A similar result has been found for other manganese compounds.¹⁴

Below about 10 kOe, the resonance frequency no longer falls on an extrapolation of the straight line, shown by the upper dashed line in Fig. 6, but rather becomes almost independent of the applied field, as indicated by the lower dashed line. The demagnetization field H_D of an infinitely long needle is $4\pi M_s \approx 9$ kOe for $(\text{LaPb})\text{MnO}_3$. For a finite cylinder, about the shape of our samples, $H_D \approx 7$ or 8 kOe. The effect on H_D when the sample consists of irregularly-shaped interacting particles is unclear. However, within the experimental errors, some form of domain structure is expected to commence forming on reducing the applied field to somewhere between 7 and 10 kOe. As H is further reduced, the domain configuration will alter to cancel in an approximate way the contribution of the applied field to the net hyperfine field. Hence ν_0 will be almost constant, as indeed was found. As the applied field approaches zero, the nuclei within domain walls will again contribute to the NMR spectra. Since ν_0 increases at $H=0$, it appears that the nuclei within the domain walls resonate at a higher frequency than those outside the walls. This conjecture is supported by noting that the structure in the NMR spectra of Fig. 2 is mainly on the high-frequency side.

The transverse relaxation time T_2 also changes when an external magnetic field is applied, increasing significantly. At least two factors are operating. First, the contribution to the relaxa-

tion time by the nuclei lying within domain walls is decreased and then eliminated as the walls are removed when the applied field is increased. The relaxation time for nuclei within a domain wall is apparently shorter than for nuclei in the bulk material. A similar conclusion has been reached recently for ^{55}Mn nuclei in manganese ferrite.²⁰ Second, the Suhl-Nakamura interaction depends on H , and leads to an increase in T_2 as the field is increased. This effect has also been detected in manganese ferrite.²⁰ Of course, it is possible that there are other field-dependent contributions to the relaxation time.

A logarithmic plot of the spin-echo amplitude against the time τ between the first two pulses, useful in the determination of T_2 , reveals a new feature, an oscillatory behavior, when an external magnetic field is present. This effect is illustrated in Fig. 7 for $\text{La}_{0.69}\text{Pb}_{0.31}\text{MnO}_3$ at $T = 77$ K. A similar spin-echo modulation has been observed before. It can be produced by the quadrupole interaction provided the magnetization makes a unique angle with the crystallographic axes,¹³ as in a single-crystal sample. For a powder this require-

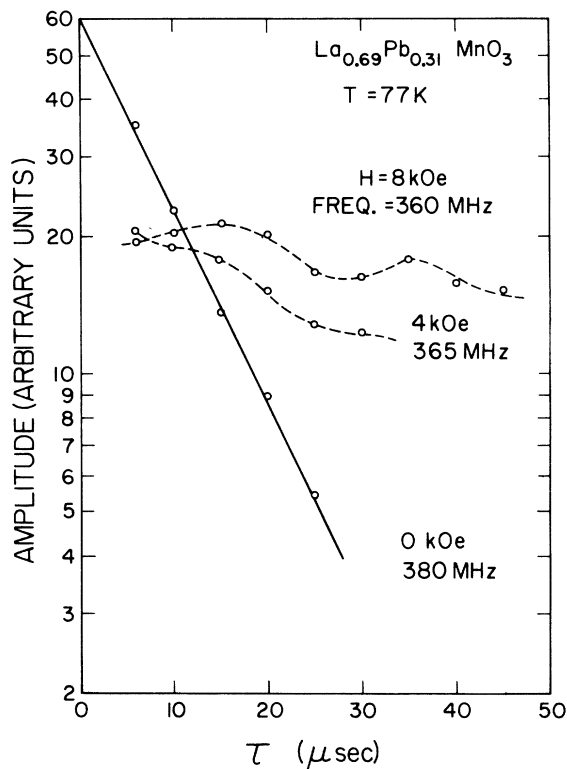


FIG. 7. Logarithmic plot of the spin-echo amplitude at the resonance frequency vs the time interval between the two applied pulses with and without the application of an external magnetic field.

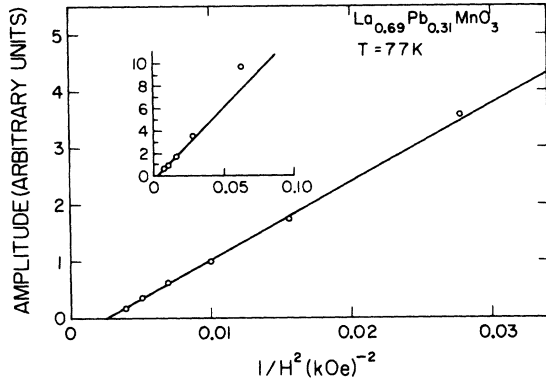


FIG. 8. Amplitude of the first echo plotted as a function of $1/H^2$ for $\text{La}_{0.69}\text{Pb}_{0.31}\text{MnO}_3$ at 77 K. The inset shows that deviations from the straight line occur at small values of field.

ment is also met if the particles rotate so that the easy axes aligned with the applied magnetic field.

Abe *et al.*¹³ have derived a relationship between the modulation period τ_m , and the quadrupole multiplet separation, $\Delta\nu_q$; they find

$$\Delta\nu_q\tau_m = 1. \quad (1)$$

From Fig. 7, $\tau_m \approx 20$ sec; hence $\Delta\nu_q = 0.05$ MHz. In addition, it can be shown from first-order perturbation theory,²¹ that

$$\Delta\nu_q = [3e^2qQ/2I(2I-1)h](m - \frac{1}{2})^2(3\cos^2\theta - 1), \quad (2)$$

where Q is the nuclear quadrupole moment, q is the electric field gradient, and θ is the angle between the direction of the hyperfine field and the axis of the electric field gradient. If θ is assumed to be zero, and with $I = m = \frac{5}{2}$, it follows that $e^2qQ/h \approx 0.17$ MHz. This quadrupole splitting is much smaller than the linewidth, and therefore cannot be observed in a steady-state experiment. Actually, in an ideal perovskite structure, the quadrupole interaction would be zero. However, $(\text{LaPb})\text{MnO}_3$ possesses a slight rhombohedral distortion¹ that presumably leads to a small electric field gradient at a ^{55}Mn nucleus.

The amplitude of the spin echo is proportional to the enhancement factor η , which represents the amplification of the applied transverse magnetic field H_x . The electronic magnetization M has the component M_x given by $M_x = M[H_x/(H + H_K - H_D)]$, where H is the static applied magnetic field and H_K is the effective crystalline anisotropy field. Since the hyperfine field H_{hf} and M are oppositely directed, the effective transverse field H_{efx} in the domain bulk is then given by

$$H_{\text{efx}} = H_x + (M_x/M)H_{\text{hf}}$$

$$= \{1 + [H_{\text{hf}}/(H + H_K - H_D)]\}H_x. \quad (3)$$

Because H_x is enhanced by the same factor during excitation and during signal emission,²² the echo amplitude enhancement η' is given by

$$\eta' = \{1 + [H_{\text{hf}}/(H + H_K - H_D)]\}^2 = (1 + \eta)^2. \quad (4)$$

From ferromagnetic resonance experiments, it is known that the anisotropy field H_K is small.³

For a sufficiently strong field, $H + H_K - H_D \approx H$ and $H_{\text{hf}}/H \approx 50$, so that Eq. (4) approximates to

$$\eta' \approx (H_{\text{hf}}/H)^2. \quad (5)$$

The amplitudes of the spin echoes are observed to decrease nonlinearly on application of an external magnetic field. For the first echo, the amplitude is linear with $1/H^2$ for sufficiently large fields, as shown in Fig. 8 for $\text{La}_{0.69}\text{Pb}_{0.31}\text{MnO}_3$ at 77 K.

At lower fields, the linear relationship breaks down as indicated in the inset to Fig. 8. Indeed, in zero field, the signal amplitude is about 35 times larger than that when $H = 14$ kOe (Fig. 5). Since no domain walls are present in the material when $H = 14$ kOe, this observation implies that in zero field the enhancement factor for the domain bulk is comparable to that for the domain walls. In other words, nuclei both within the domain walls and within the domain bulk make significant contributions to the absorption spectra when no external magnetic field is present.

IV. NMR SPECTRA OF $\text{La}_{1-x}\text{Pb}_x\text{Mn}_{1-y}\text{Fe}_y\text{O}_3$

Polycrystalline samples of $\text{La}_{1-x}\text{Pb}_x\text{Mn}_{1-y}\text{Fe}_y\text{O}_3$ were made by starting with the relevant oxides and using ceramic techniques, as described earlier.⁴ The Curie temperatures ranged from 252 K for $x = 0.44$ and $y = 0.03$ to 176 K for $x = 0.44$ and $y = 0.17$. As a result the spin-echo signal was harder to detect; it was not observable even at $T = 4.2$ K for the highest iron dopings, viz., $y \geq 0.15$. Most of the data were collected at 1.6 K, the lowest temperature attainable with the apparatus. NMR spectra for ^{55}Mn in $\text{La}_{0.70}\text{Pb}_{0.30}\text{Mn}_{1-y}\text{Fe}_y\text{O}_3$ are shown in Fig. 9 for $y = 0.03, 0.10$, and 0.15 at $T = 1.6$ K and for $y = 0.03$ at $T = 4.2$ K. The central peak, which occurs at about 382 ± 5 MHz appears to correspond to the resonance frequency observed with $y = 0$, as listed in Table I. The peak on the high-frequency side at about 421 MHz is attributed to Mn^{3+} ions for the following two reasons. First, a peak at about 420 MHz in the NMR spectra of manganese ferrite has been identified with Mn^{3+} ions.²³ Second, the frequency, 421 MHz, lies close to an extrapolation of the linear ν_0 -vs- x curve to $x = 0$ (see Fig. 3). The peak at about 332 MHz on the low-frequency side in Fig. 9 is attributed to Mn^{4+} ions for similar reasons. First,

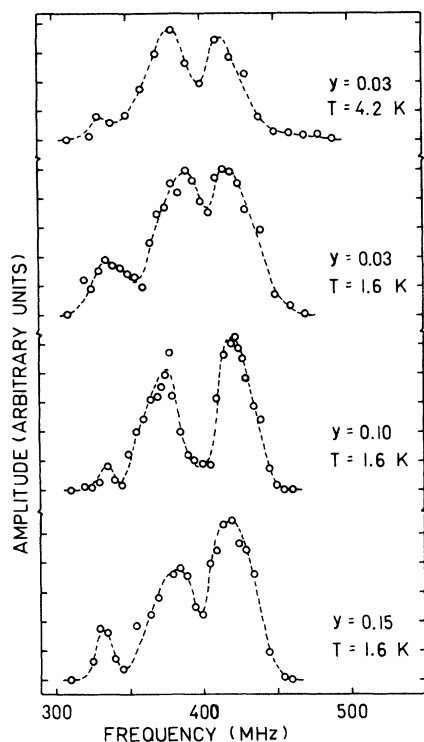


FIG. 9. NMR spectra of $\text{La}_{0.70}\text{Pb}_{0.30}\text{Mn}_{1-y}\text{Fe}_y\text{O}_3$.

a resonance at about 310 MHz for a lithium-manganese ferrite has been identified with Mn^{4+} ions.¹⁴ Second, a linear extrapolation to $x = 1.0$ in Fig. 3 lies below but close to 332 MHz. It is interesting to note also that for $\text{La}_{1-x}\text{Ca}_x\text{MnO}_3$ with $x = 0.15$, Matsumoto⁹ associates a peak at 323 MHz with Mn^{4+} ions and that another peak occurs at 411 MHz.

From the Mn^{3+} line position, and with $\langle S \rangle = 2$, it follows that the hyperfine constant $|A|$ is $7.0 \times 10^{-3} \text{ cm}^{-1}$ and the hyperfine field H_{hf} is -393 kOe . From the Mn^{4+} resonance frequency, and with $\langle S \rangle = 1.5$, it is found that $|A| = 7.4 \times 10^{-3} \text{ cm}^{-1}$ and $H_{\text{hf}} = 309 \text{ kOe}$. A quite different technique provides comparative values for A ; ESR experiments yield $|A| = 7.2 \times 10^{-3} \text{ cm}^{-1}$ for Mn^{4+} in TiO_2 ,²⁴ and $|A| = 7.0 \times 10^{-3} \text{ cm}^{-1}$ for Mn^{4+} in Al_2O_3 .¹⁵

On the basis of earlier experiments on $\text{La}_{1-x}\text{Pb}_x\text{Mn}_{1-y}\text{Fe}_y\text{O}_3$ in which other techniques were employed, an energy-level diagram was proposed.⁴ It is known that the $3d$ electrons of ferric ions tend to be more localized than those for Mn^{3+} ions. It was suggested that the Fe^{3+} ions have well-localized ${}^6A_{1g}$ states lying about 2.5 eV below the Fermi level of the narrow σ^* conduction band formed by the e_g electrons of the Mn^{3+} ions. The transfer of an electron from a Mn^{3+} to a Fe^{3+} ion nearest neighbor then is the origin of the antiferro-

magnetic superexchange interaction. On the basis of this energy diagram, a phenomenological theory of the Curie temperature was developed.⁴ It was concluded that the Curie temperature decreases as the iron doping increases because (a) the number of electrons in the σ^* band decreased, and (b) the transfer integral decreased.

The NMR spectra provide evidence that spin oscillations occur at manganese ions, presumably most likely when a ferric ion is the nearest neighbor. Thus, the number of electrons in the σ^* band is further reduced. In addition, this effect would contribute to the decrease in the transfer integral. The probability for the trapping of a hole or an electron at Mn^{4+} and Mn^{3+} ions, respectively, should be related in a simple way to the iron concentration. The peak intensities, shown in Fig. 9, do indicate this trend; the data are however not sufficiently accurate to permit a quantitative analysis. Further, the trapping probability would be expected to increase as the temperature is lowered; the data for $y = 0.03$ at $T = 4.2$ and 1.6 K (Fig. 9) provided qualitative support for this expectation. Further investigations may permit a detailed model for the spin- and charge-density oscillations, perhaps along the lines of that used for doped magnetite,²⁵ to be developed for the iron-doped manganites.

Matsumoto, in his experiments on $(\text{La}_{1-x}\text{Ca}_x)\text{MnO}_3$ for $x < 0.15$,⁹ found similar evidence for electron and hole localization, and accounted for his results by postulating d -hole trapping in the neighborhood of a Ca^{2+} ion. It is possible that a similar process occurs near the Pb^{2+} ions; however no evidence for this effect is found for $\text{La}_{1-x}\text{Pb}_x\text{MnO}_3$ ($y = 0$) when $0.25 < x < 0.45$. There seems to be no reason to believe that such trapping is important when $y \neq 0$, at least for the range of x values used in the present investigation.

The relaxation time is decreased in iron-doped compounds. For example, at $T = 1.6 \text{ K}$, and over the frequency range from 325 to 425 MHz, it is found that T_2 varies between 10 and $30 \mu\text{sec}$ for $y = 0.03$, and between 4 and $12 \mu\text{sec}$ for $y = 0.10$ and 0.15 . Some variation of T_2 with frequency is indicated. However, in view of the small value of the relaxation time, and the experimental uncertainties, the data do not allow significant inferences to be made at this time.

V. SUMMARY

Oscillations in the spin-echo amplitude when the time between the two applied pulses is varied indicate the presence of a quadrupole interaction at the ${}^{55}\text{Mn}$ nuclei in $\text{La}_{1-x}\text{Pb}_x\text{MnO}_3$. Since Mn^{3+} is a Jahn-Teller ion, a distortion of the surrounding oxygen octahedron is expected,²⁶ and would lead

to an electric field gradient. The quadrupole interaction appears to be responsible for the $2I$ (or fewer) echoes observed. Measurements of the spin-spin relaxation time T_2 seem to imply that the Suhl-Nakamura interaction is also important, at least for temperatures at and below 4.2 K. Experiments with an external magnetic field applied yield a nuclear gyromagnetic ratio consistent with literature values. The NMR absorption lines are the sum of two components, one from nuclei inside and the other from nuclei outside the domain walls; the latter component is expected to be appreciable because the crystalline anisotropy is known to be small. Future experiments in which the line shape and the relaxation time are determined more accurately may permit resolution of these two components.

For $\text{La}_{1-x}\text{Pb}_x\text{Mn}_{1-y}\text{Fe}_y\text{O}_3$, the NMR spectra provide convincing evidence for increased electron localization at the manganese ions, and thus per-

mit further insight on the associated magnetization properties. The absence of these absorptions for $y=0$ stresses the importance of the double-exchange conduction band in producing a motionally narrowed state intermediate between the Mn^{3+} and Mn^{4+} ions. Information on the electron energy levels, and hence the interactions in $(\text{LaPb})\text{MnO}_3$, are of particular relevance at this time because this material has potential use as a catalyst²⁷ for the oxidation of pollutants present in the exhausts from vehicles such as automobiles.

ACKNOWLEDGMENTS

We wish to thank A. Hirai of Kyoto University and C. W. Searle for some valuable contributions to this study. We are grateful to the Defense Research Board and to the National Research Council of Canada for supporting this project financially.

*Present address: Dept. of Applied Science, Hong Kong Polytechnic, Hung Hom, Kowloon, Hong Kong.

¹A. H. Morrish, B. J. Evans, J. A. Eaton, and L. K. Leung, *Can. J. Phys.* **47**, 2691 (1969).

²L. K. Leung, A. H. Morrish, and C. W. Searle, *Can. J. Phys.* **47**, 2697 (1969).

³C. W. Searle and S. T. Wang, *Can. J. Phys.* **47**, 2705 (1969); S. T. Wang and C. W. Searle, *ibid.* **49**, 387 (1971).

⁴L. K. Leung, A. H. Morrish, and B. J. Evans, *Phys. Rev. B* **13**, 4069 (1976).

⁵C. W. Searle and S. T. Wang, *Can. J. Phys.* **48**, 2023 (1970); K. Kubo and J. Ohata, *J. Phys. Soc. Jpn.* **33**, 21 (1972).

⁶See, for example, C. Zener, *Phys. Rev.* **82**, 403 (1951); P. W. Anderson and H. Hasegawa, *ibid.* **100**, 675 (1955); P. G. de Gennes, *ibid.* **118**, 141 (1960).

⁷S. F. Alvarado, W. Eib, P. Munz, H. C. Siegmann, M. Campagna, and J. P. Remeika, *AIP Conf. Proc.* **29**, 664 (1976); *Phys. Rev. B* **13**, 4918 (1976).

⁸G. Matsumoto and S. Iida, *J. Phys. Soc. Jpn.* **21**, 2734 (1966).

⁹G. Matsumoto, *J. Phys. Soc. Jpn.* **29**, 615 (1970); *IBM J. Res. Dev.* **14**, 258 (1970).

¹⁰C. W. Searle and J. Davis, *Phys. Rev. Lett.* **27**, 1380 (1971); J. H. Davis and C. W. Searle, *Phys. Rev. B* **9**, 323 (1974).

¹¹L. K. Leung, Ph.D. thesis (University of Manitoba, 1972) (unpublished).

¹²I. Solomon, *Phys. Rev.* **110**, 61 (1958).

¹³H. Abe, H. Yasuoka, and A. Hirai, *J. Phys. Soc. Jpn.* **21**, 77 (1966).

¹⁴T. Kubo, H. Yasuoka, and A. Hirai, *J. Phys. Soc. Jpn.* **21**, 812 (1966).

¹⁵G. Geschwind, P. Kisluik, M. P. Klein, J. P. Remeika, and D. L. Wood, *Phys. Rev.* **126**, 1648 (1962).

¹⁶M. Nakada, K. Awazu, S. Ibuki, Y. Miyako, and M. Date, *J. Phys. Soc. Jpn.* **19**, 781 (1964).

¹⁷H. Y. Carr and E. M. Purcell, *Phys. Rev.* **94**, 630 (1954).

¹⁸J. M. Winter, *Phys. Rev.* **124**, 452 (1961).

¹⁹H. Suhl, *Phys. Rev.* **109**, 606 (1958); T. Nakamura, *Prog. Theor. Phys.* **20**, 547 (1958).

²⁰J. H. Davis and C. W. Searle, *Phys. Rev. B* **14**, 2126 (1976).

²¹A. Abragam, *The Principles of Nuclear Resonance* (Oxford U. P., Oxford, 1961).

²²A. J. Heeger and T. W. Houston, *Phys. Rev.* **135**, A661 (1964).

²³T. Kubo, A. Hirai, and H. Abe, *J. Phys. Soc. Jpn.* **26**, 1094 (1969).

²⁴H. G. Andersen, *Phys. Rev.* **120**, 1606 (1960).

²⁵C. Boekma, F. van der Woude, and G. A. Sawatzky, *Proceedings of the Fifth International Conference on Mössbauer Spectroscopy* (Czechoslovakian Atomic Energy Commission, Prague, 1975), pp. 96-98.

²⁶G. Matsumoto, *J. Phys. Soc. Jpn.* **29**, 606 (1970).

²⁷L. A. Pedersen and W. F. Libby, *Science* **176**, 1355 (1972); R. J. H. Voorhoeve, J. P. Remeika, and D. W. Johnson, *ibid.* **180**, 62 (1973).